

## Gamma-Ray Measurements with a Magnetic Lens Spectrometer

W. F. HORNYAK, T. LAURITSEN, AND V. K. RASMUSSEN

*Kellogg Radiation Laboratory, California Institute of Technology, Pasadena, California*

(Received May 16, 1949)

Effects of instrument resolution and converter thickness on photoelectron lines have been investigated experimentally for gamma-radiation from 0.4 to 3 Mev. While determinations based on the high energy extrapolated edge of the lines seem to require no corrections for converter thicknesses, the peak value, which does require corrections, is in some cases more easily located. Peak shifts determined for thorium converters near 0.5 Mev are extrapolated to other energies by use of theoretical arguments. Values based on both types of determinations are quoted for gamma-radiation from the reactions  $\text{Li}^7(p,p')\text{Li}^{7*}$ ,  $\text{Be}^9(d,n)\text{B}^{10*}$ , and  $\text{Co}^{60}(\beta^-)\text{Ni}^{60*}$ . The corresponding excited level transition energies obtained are  $\text{Li}^{7*}$ :  $476.7 \pm 0.9$  kev;  $\text{B}^{10*}$ :  $713.8 \pm 1.3$  kev;  $\text{Ni}^{60*}$ :  $1172.4 \pm 1.8$  kev and  $1330.9 \pm 2.1$  kev.

THE comparatively large aperture and high resolution of the magnetic lens beta-ray spectrometer have led to its increasing application to the precise determination of gamma-ray energies in the range from a few tens of kilovolts to several Mev. The most common method used consists in observing the spectrum of photoelectrons produced by the gamma-radiation either by internal conversion in the source or by external conversion in a suitable foil. In both cases, essentially monochromatic lines are observed, broadened, and displaced to varying degrees depending on the energy losses in the source or converter and on the resolution of the instrument. We have attempted to make a systematic examination of these effects as they apply to the determination of certain gamma-ray energies in the region from 0.4 to 3 Mev.

### APPARATUS

The spectrometer used in this work was patterned after the instrument described by Deutsch, Elliott, and Evans,<sup>1</sup> modified to use the annular focusing discussed by Frankel and others.<sup>2</sup> It comprises a brass tube 10" in diameter and 48" long (Fig. 1) in which are placed suitable baffles to limit the electron trajectories and to reduce scattering and direct radiation background. A helical baffle is provided to permit distinction between positive and negative electrons. The focusing magnetic field is produced by four individual water-cooled coils which were in the present experiments grouped together at the middle of the tube. Since the magnetic circuit contains no iron, the field is proportional to the current. As a measure of the current in the spectrometer coils, the millivolt reading on a Type K Leeds and Northrup potentiometer in conjunction with a set of carefully intercalibrated Manganin shunts was used. The unbalanced output of the potentiometer was simultaneously indicated on a sensitive galvanometer and amplified as an a.c. signal after being changed into a square wave at a low signal level by a Western Electric sealed pressure relay. This amplified

signal was used to control a  $\frac{1}{2}$ -K.W. amplidyne in the field circuit of the 60-K.W. generator supplying the spectrometer current. The spectrometer current was held to better than 2 parts in 10,000 on the average.<sup>3</sup>

A vacuum connection to a 1.4-Mev electrostatic accelerator enabled suitable targets at the source position to be bombarded by high energy protons or deuterons for the study of prompt and short-lived radioactive gamma-radiation. Gamma-rays produced at the source position ejected secondary electrons from a heavy element converter immediately adjacent. A schematic diagram of the source assembly is shown in Fig. 2. The source and converter were supported by an 0.02 inch wire and the region around the source was completely free of scattering materials for a minimum of three inches. Particular care was taken to reproduce accurately the centering and axial locations of the sources and, while the diversity in the nature of the gamma-ray sources required some variation in techniques, the geometry of the source assembly was standardized as much as possible.

The internal parts of the spectrometer were centered with respect to the tube at assembly. Further adjustment of the geometrical alignment was made by moving the tube with respect to the axis of the coils in such a way as to maximize the observed intensity of the high energy internal conversion "X" line ( $B\rho=10,000$  gauss cm) of ThD. Stray lateral magnetic fields were then compensated, by means of two large, mutually perpendicular coils, to give maximum intensity for the comparatively low energy "F" line from ThC ( $B\rho=1385$  gauss cm), the "I" line ( $B\rho=1750$  gauss cm) being used as an auxiliary check. It was observed that when the compensation was properly set, the instrument resolution was the same for all of the internal conversion lines. When the compensation was incorrect the first sign of maladjustment was a line broadening and loss in intensity which was progressively worse the lower the line energy. Only after a considerable amount of maladjustment of the compensation were the line shapes

<sup>1</sup> Deutsch, Elliott, and Evans, *Rev. Sci. Inst.* **15**, 178 (1944).

<sup>2</sup> S. Frankel, *Phys. Rev.* **73**, 804 (1948); J. M. DuMond, *Rev. Sci. Inst.* **20**, 160 (1949); Persico, *ibid.*, 191.

<sup>3</sup> We are indebted to Mr. G. W. Downs for much helpful advice on this control system and to Messrs. C. B. Dougherty and W. D. Gibbs for putting it into operation.

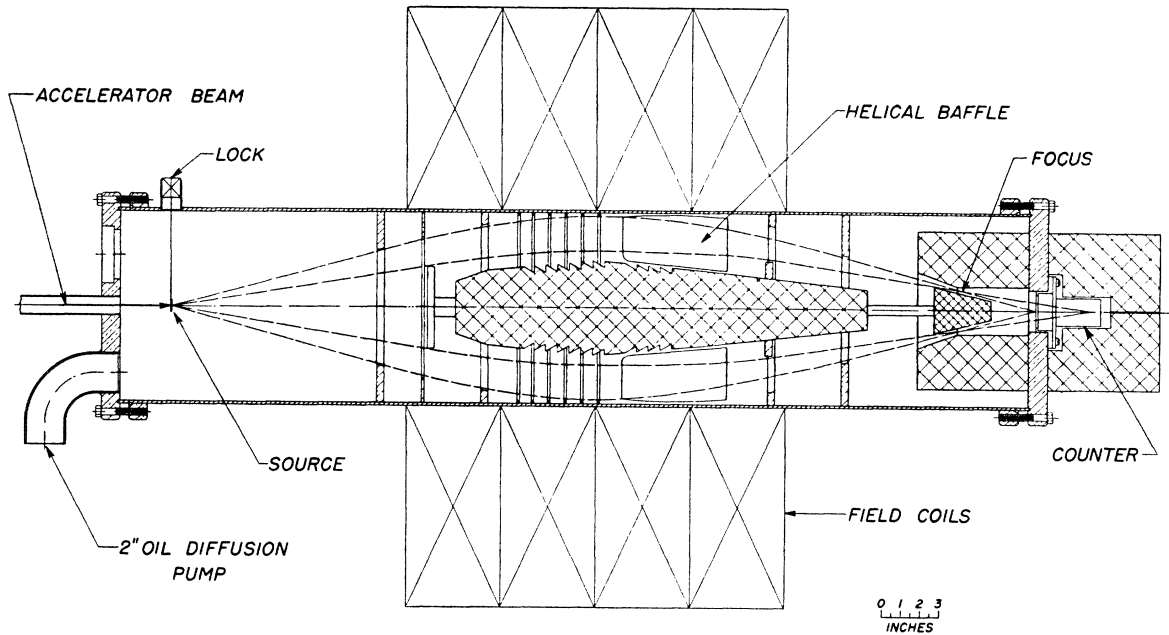


FIG. 1. Spectrometer assembly.

asymmetrical or noticeably shifted. Because the component of stray field parallel to the spectrometer axis was not compensated, a small correction to the observed line position was made. For the arrangement used here, this correction is

$$\delta \text{M.V.}/\text{M.V.} = 22S/B\rho,^4$$

where  $S$  is the axial component of the stray field in gauss,  $B\rho$  the momentum of the line in gauss cm, and M.V. is the millivolt reading on the potentiometer in-

dicating the spectrometer coil current. Since in this experiment a value of  $S = 0.30 \pm 0.1$  gauss was measured, the correction at 2000 gauss cm, for example, is 0.3<sub>3</sub> percent.

In the final configuration, the spectrometer yielded a symmetric curve, with a shape well approximated by a Gaussian function (Fig. 3) of width at half maximum of 1.5<sub>2</sub> percent. In general this width will depend on the instrument aperture arrangement and the source size. An investigation showed that for the range of source sizes used here, the line shapes were comparatively independent of source size. The solid angle is estimated to be 0.5 percent of a sphere.

#### GAMMA-RAY MEASUREMENTS: INTERNAL CONVERSION

Internal conversion photoelectrons provide a particularly simple indication of the gamma-ray energy, if the available intensity is great enough to permit the use of a source of such thickness that the energy loss of the electrons may be ignored. In such cases, the observed electron distribution is simply the "window" or resolution curve of the instrument and the determination may be made directly in terms of either the peak or the extrapolated edge positions. Comparison with a known line of the same character then provides the calibration. As an example of this technique, and for a calibration required for subsequent work we have made an intercomparison of the internal conversion lines of the gamma-radiation of ThD ( $X$  line) and Au<sup>198</sup> ( $K$  and  $L$  lines). The former line was measured by Ellis<sup>5</sup> in terms of the  $I$  line for which he obtained an absolute value by measurement of the magnetic field.

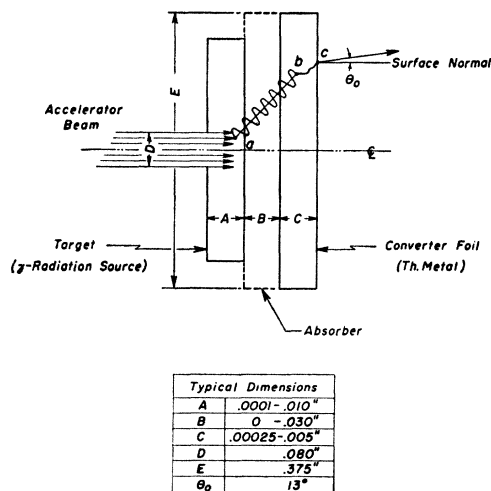


FIG. 2. Schematic drawing of source assembly.

<sup>4</sup> The dimensional constant 22 is for a configuration: source to counter distance = 114 cm; full width at half maximum of axial component of focusing field = 53 cm; maximum radial electron excursion for median ray = 10 cm; acceptance angle for median ray = 13°.

<sup>5</sup> Ellis, Proc. Roy. Soc. A138, 318 (1932).

Siegbahn<sup>6</sup> measured the absolute values of the  $I$  and  $F$  lines by comparing the difference with x-ray spectroscopic values and obtained momenta on the average 0.11 percent lower than those given by Ellis. Taking the mean of the two  $I$  line determinations and using Ellis'  $X/I$  ratio, one obtains a momentum value of  $10,000 \pm 14$  gauss cm, or  $2.618 \pm .004$  Mev for the gamma-ray energy.<sup>7</sup>

The gamma-radiation of  $\text{Au}^{198}$  has been measured in a curved crystal spectrometer by DuMond, Lind and Watson<sup>8</sup> who give  $411.2 \pm 0.1$  kev for the energy, yielding values of  $B\rho = 2219.7$  gauss cm for the  $K$  conversion line and  $B\rho = 2502.1$  gauss cm for the  $L$  line. The  $K$  and  $L$  binding energies used here were determined from the critical absorption wave-length table of Compton and Allison.<sup>9</sup> Since the  $L_I$ ,  $L_{II}$ , and  $L_{III}$  lines were not resolved, a weighted mean value for the  $L$  shell energy was used. Table I gives the pertinent values for the elements used in these experiments.

For the "X" line measurements, sources of  $\sim 4$  mm diameter of ThB were prepared by electrostatic collection from Tn gas on .0005-inch Al foils. The thin (essentially mono-molecular) deposits so obtained were covered by an additional layer of .0005 inch Al foil to prevent recoil ThC'' nuclei from escaping. The  $\text{Au}^{198}$  source was plated from solution on a .0005 inch Cu foil and had a thickness of less than 0.1 mg/cm<sup>2</sup>.<sup>10</sup> The total activity of these sources was of the order of 20  $\mu$  curies. Typical curves obtained are reproduced in Fig. 3 and Fig. 4, and the resulting peak and edge calibration values in terms of millivolts drop across a standard shunt presented in Table II.<sup>11</sup> The indicated locations of the  $X_a$  and  $X_{a1}$  lines in Fig. 3 are calculated from Ellis' data. The close agreement of the calibrations attests to the accuracy of the method and provides a relative check on the two independent standards.<sup>12</sup>

Measurements were also made on the ThF and I lines, but the uncertainties in the stray magnetic field corrections limited the precision to about 0.5 percent. The values obtained were in agreement with the ratios quoted by Ellis within this accuracy.

<sup>6</sup> Siegbahn, Arkiv f. Ast. Math. Fys. **30A**, No. 20 (1944).

<sup>7</sup>  $B\rho = (10^4/2.99776)[E(E+1.02158)]^{1/2}$ ;  $E$  in Mev (absolute).

<sup>8</sup> DuMond, Lind, and Watson, Phys. Rev. **73**, 1392 (1948).

<sup>9</sup> Compton and Allison, *X-Rays in Theory and Experiment* (Van Nostrand Company, Inc., New York, 1935). p. 794.

<sup>10</sup> We are indebted to the AEC for their cooperation in supplying the  $\text{Au}^{198}$  and  $\text{Co}^{60}$  sources and to Mr. J. H. Sullivan for the chemical preparations involved in certain of the applications.

<sup>11</sup> The focusing current for lines having momenta greater than 4500 gauss cm was measured on a shunt having .1330<sub>3</sub> times the resistance of the standard shunt.

<sup>12</sup> If one uses the peak calibration for the  $\text{Au}^{198}$  to determine the  $X$  line value from this experiment, a value of 9998 gauss cm is obtained, corresponding to a gamma-ray energy of 2.618 Mev with a probable error of 4 kev. The corresponding extrapolated edge value, which is in this case considered somewhat less reliable because of the overlapping with the  $X_a$  line, yields  $B\rho = 9989$  gauss cm or 2.615 $\pm$ .006 Mev. This comparison has been recently repeated with a resolution of 1.0%, resulting in a  $B\rho$  value of 9982 gauss cm for the  $X$  line peak or an energy of 2.613 $\pm$ .004 Mev.

TABLE I.  $K$  and  $L$  shell energies.

Element	$E_K$ (kev)	$E_{L_I}$ (kev)	$E_{L_{II}}$ (kev)	$E_{L_{III}}$ (kev)	$\bar{E}_L$ (kev)
Thorium	109.8	20.5	19.7	16.3	20.1
Lead	88.0	15.8	15.2	13.0	15.6
Mercury	83.1	14.8	14.2	12.3	14.5
Nickel	8.3 <sub>4</sub>	—	—	—	—

#### EXTERNAL CONVERSION MEASUREMENTS

For gamma-ray sources in which no appreciable internal conversion occurs, photoelectrons may be produced in an external converter of high atomic number, using the arrangement of Fig. 2. Radiation produced in the target as at  $a$  in the figure will undergo photoelectric conversion throughout the volume of the converter foil. One such process is schematically illustrated at  $b$ ; the photoelectron so produced will then emerge from the foil at some point  $c$  after having followed a path determined by a comparatively large number of small angle elastic scatterings, resulting principally from the interaction of the photoelectron with the nuclear coulomb fields of the converter atoms. At the same time, the photoelectron suffers ionization loss by interaction with the electrons in the converter, resulting in its emergence at  $c$  with a total loss of energy determined by the path length  $b-c$ . Because of the effects of scattering and straggling in the foil, the number of electrons emerging in a given energy interval will decrease as the energy loss increases, leading to a spectrum with a maximum value for zero energy loss, tailing off monotonically toward lower energies at a rate determined by the initial photoelectron energy and the converter thickness and atomic number. The observation of such a distribution with an instrument of finite resolution will in general result in a shifting of the peak and extrapolated front edge of the curve by a magnitude depending on the resolution and on the exact shape of the spectrum.

To illustrate the effect of converter thickness on line shape at a comparatively low energy, experimental

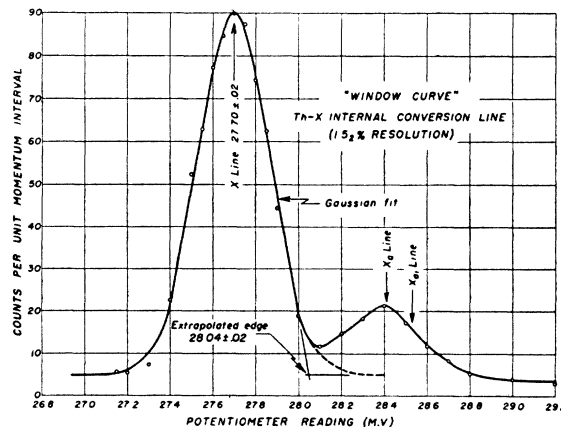


FIG. 3. "Window curve": observed spectrum from internal conversion lines of 2.62 Mev gamma-radiation of ThD.

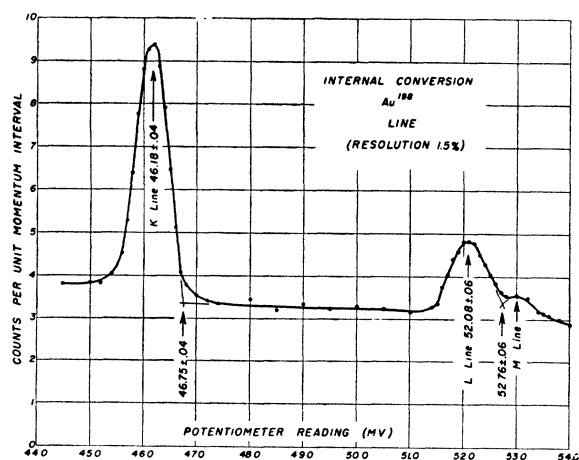


FIG. 4. Internal conversion lines of 411 keV gamma-radiation of  $\text{Au}^{198}$ .

curves of the  $K$  conversion in thorium foils of the 411.2 keV gamma-radiation of  $\text{Au}^{198}$  are shown in Fig. 5. The source used for this work consisted of a 1 mm square of activated Au foil .001 inch thick placed on the back of a .030 inch copper absorber, to which were attached the thorium foils.<sup>13</sup> The copper absorber was used to suppress the continuous  $\beta$  radiation. The ordinates of the various curves have been adjusted only to the extent that backgrounds of the order of 30 percent, due partly to the tailing of the  $L$  and  $M$  lines at  $\approx 51$  M.V. and partly to general radiation, have been subtracted. The intensities plotted are for a constant source strength in all cases.

Perhaps the most significant feature of these curves, from the standpoint of their usefulness in energy determinations, is the observation that the intersection of the extrapolated front edge with the background is apparently independent of converter thickness. A similar set of curves for the 717 keV gamma-radiation from the reaction  $\text{Be}^9(d,n)\text{B}^{10*}$  is shown in Fig. 6. The curves of Fig. 7 illustrate the two high energy gamma-rays accompanying the decay of  $\text{Co}^{60}$ , where the background has not been subtracted.<sup>14</sup> In all cases the extrapolated edge values for the  $K$  conversion lines were found to be independent of converter thickness to within about 0.2 percent. Reference to Table III shows that the value of the  $\text{Au}^{198}$  gamma-ray deduced from the extrapolated edge agrees within 0.1 keV with the known value (using extrapolated edges of the internal conversion lines referred to above for calibration).

<sup>13</sup> Throughout this paper the converter thicknesses quoted in inches are nominal thicknesses. By weighing these have been determined to be:

.00025 inches	7 mg/cm <sup>2</sup>
.0005 inches	16 mg/cm <sup>2</sup>
.001 inches	25 mg/cm <sup>2</sup>
.002 inches	57 mg/cm <sup>2</sup>
.003 inches	78 mg/cm <sup>2</sup>
.004 inches	113 mg/cm <sup>2</sup>
.005 inches	150 mg/cm <sup>2</sup>

<sup>14</sup> The cobalt curves were run with only .001 inch Cu absorber: the abnormal intensity of the  $L$  lines is due to the superposition on them of the internal conversion  $K$  lines, shifted by the energy loss in the absorber.

The height and location of the peaks and the magnitude of the low energy side of the distributions, on the other hand, are clearly affected by changes in the converter thickness. Between the .00025 inch and the .0005 inch curves in Fig. 5, one observed an increase of intensity and a shift of the maximum toward lower energy. As compared with the expected peak for zero converter thickness, the .00025 inch peak is shifted by 1.7 keV and the .0005 inch by 3.2 keV. For thicknesses greater than .0005 inch one observes no further shift or increase in peak intensity (the intensity actually decreases somewhat because of the absorption of the gamma-radiation) and only the lower energy tail seems to be affected.

In an effort to ascertain the primary distribution of the electrons emerging from the converter, the experimental curves of Fig. 5 have been "unfolded," i.e., the effect of finite resolution removed, by a method of successive approximations assuming a Gaussian window shape. Although such a procedure cannot in general be expected to reveal changes occurring in intervals small compared to the resolution width (7.3 keV), in this case the unfolding was facilitated by the fact that the upper limit of the primary spectrum was known absolutely from the calibration. The curves of Fig. 8, which exhibit the inferred spectra for three converter thicknesses, show that the number of electrons per unit momentum interval emerging from the converter drops very sharply in less than  $\sim 3$  keV and thereafter falls more gradually at a rate depending on converter thickness. The ordinates in these curves are in the same (arbitrary) units as those of Fig. 5, to facilitate comparison. As a check on the reliability of the inferred primary distribution, the .0005 inch converter curve was repeated at a resolution of 0.65 percent, using a smaller source, and introducing several other modifications in the spectrometer. The primary spectrum representing the best fit for the two resolutions is shown in Fig. 9, where the numerically integrated "folds" with Gaussians of 0.65 percent and 1.5 percent width are also shown, together with the experimental points. This inferred distribution agrees well with the corresponding one in Fig. 8: the initial decrease in the number of electrons per unit energy interval is again very pronounced. The unfolding of several other curves obtained from 0.7 and 1.1 MeV gamma-rays has yielded similar shapes. While the present experiments appear to indicate that the character of the primary spectrum undergoes an abrupt change in the neighborhood of two to four keV energy loss (for the  $\text{Au}^{198}$  radiation), it should be pointed out that the unfolding process is necessarily quite sensitive to small experimental errors; an upward shift of the assumed front edge of the primary spectrum of 0.5 keV—about the probable error—yields a satisfactory fit with a distribution function dropping off to half the maximum value in four to six keV and consequently with a considerably less abrupt

TABLE II. Calibration lines.

Line	$E_\gamma$ (keV)	$E_e$ (keV)	$B\rho$	Edge† M.V.	Peak† M.V.	( $B\rho$ /M.V.) edge	( $B\rho$ /M.V.) peak
ThD K	2618 ±4	2530	10,000	211.10*	208.64*	47.37 <sub>0</sub>	47.92 <sub>9</sub>
Au <sup>198</sup> decay K	411.2±.1	328.1	2,219.7	46.89	46.32	47.33 <sub>8</sub>	47.92 <sub>1</sub>
Au <sup>198</sup> decay L	411.2±.1	396.7	2,502.1	52.90	52.22	47.29 <sub>9</sub>	47.91 <sub>5</sub>
					Calibration**:	47.34 <sub>9</sub> ±.03	47.92 <sub>5</sub> ±.03

† Corrected for axial component of stray field.  
 \* Including 9 gauss cm correction for cover foil; reduced to standard shunt readings.  
 \*\* ThD values weighted 3X; mean of three runs given in table.

change in slope. More definite information on the exact shape of the primary spectrum in the first few kilovolts must clearly be sought in further experiments employing significantly higher resolution. In any case, it is clear that there exists near the high energy limit of the spectrum a considerable excess of electrons over what might be expected if scattering and straggling effects were neglected and that the common assumption of a rectangular distribution may be quite misleading in this energy region. It is presumably just the existence of this large number of electrons with small energy loss which accounts for the fact that the extrapolated edge of the distribution observed with the resolutions used here is relatively independent of converter thickness. With a considerably broader window curve, one might expect the influence of the back slope to become relatively more important, resulting in a detectable edge shift.

The behavior of the distribution as a function of energy was studied using K photoelectrons produced in a .0005-inch thorium foil by the following gamma-rays:

- (a) Au<sup>198</sup> radiation (411.2 keV)—.030 inch Cu absorber and .0005 inch Th converter.
- (b) Li<sup>7\*</sup> radiation (478 keV)—produced by bombardment of a Li target by protons: same absorber and converter.
- (c) Annihilation radiation (510.8 keV)—from 10 min N<sup>13</sup> produced by bombarding a .010 inch thick graphite target with deuterons; same absorber and converter.
- (d) B<sup>10\*</sup> (717 keV)—produced in the reaction Be<sup>9</sup>(d n)B<sup>10\*</sup> by deuteron bombardment of an .004 inch Be target with the .0005 inch Th converter only.

The observed spectra are illustrated in Fig. 10, where the momentum scales have been adjusted by multiplication to bring the front edges into coincidence. The location  $B\rho/B\rho_0=1.000$  corresponds to the true position of the photoelectron line, determined absolutely for the Au<sup>198</sup> radiation. In Table III, the gamma-ray energies derived from the observed extrapolated front edges are presented, including the Co<sup>60</sup> determinations from Fig. 7.

An independent check on the consistency of the data and support for the assumption that the extrapolated front edge does not, within the present uncertainty, require correction for converter thickness is provided by the close agreement of the observed value of the annihilation radiation to the known figure of 510.8 keV.<sup>15</sup> The probable errors indicated include estimates of uncertainties in matching the curves and subtracting

background in addition to such systematic errors as appear in current measurement, source location and stray field corrections.

Examination of the curves of Fig. 10 shows that, as the energy is increased, the tail of the distribution becomes less prominent compared to the resolution of the instrument, which is given by a constant width on this plot. The peak locations for the four curves are identical within the experimental error of about 0.1 percent and indicate a displacement downward of 0.66 percent in momentum. That the peaks coincide in this case is to some extent fortuitous; a thinner converter would be expected to give a relatively smaller shift at the higher energy (compare Fig. 11).

PEAK SHIFT CORRECTIONS

It would appear from these experiments that, as long as variations in source diameter sufficient to affect the window curve are avoided, the extrapolated edge determination is to be preferred because of its relative independence of converter thickness. However, in many practical cases, uncertainties in the background and the interference of neighboring lines may make such deter-

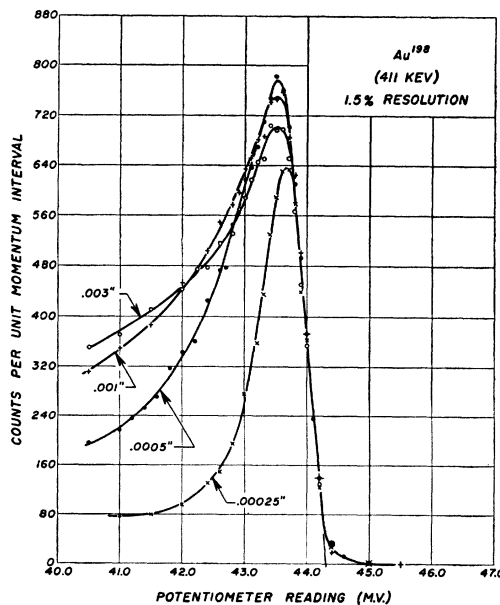


FIG. 5. 411 keV radiation of Au<sup>198</sup>, converted in various thorium foils.

<sup>15</sup> DuMond and Cohen, Rev. Mod. Phys. 20, 82 (1948); DuMond, Lind, and Watson, Phys. Rev. 75, 1226 (1949).

TABLE III. *K*-line extrapolated edge determinations—.0005-inch thorium converter.

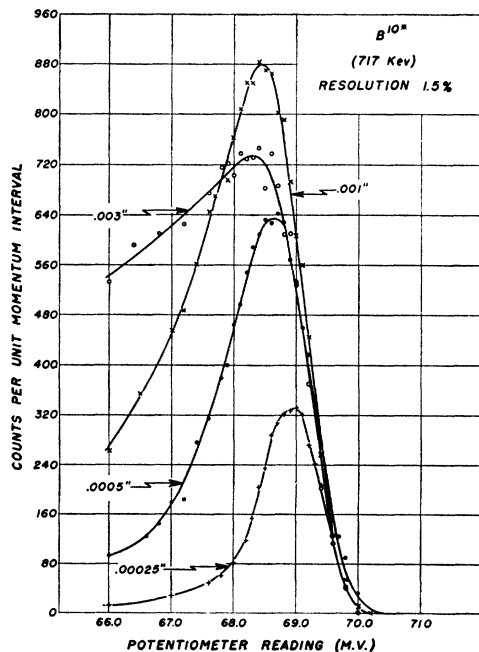
$\gamma$ -Ray source	M.V.† (current)	$B\rho$ †† (gauss-cm)	$E_e$ (kev)	$E_e + E_k$ (kev)
Au <sup>198</sup> decay	44.48	2106.1	301.3	411.1 ± .6
Li <sup>7*</sup>	50.42	2387.3	368.5	478.3 ± .7
e <sup>+</sup> annihilation	53.21	2519.4	401.0	510.8 ± .7
B <sup>10*</sup>	70.04	3316.3	606.9	716.7 ± 1.0
Co <sup>60</sup> decay (a)	104.8 <sub>6</sub> } ††	4965	1062.8	1172.8 ± 2.5
Co <sup>60</sup> decay (b)	116.5 <sub>4</sub> }	5518	1220.4	1330.2 ± 2.9

† Corrected for axial component of stray field.

†† Values reduced to standard shunt readings.

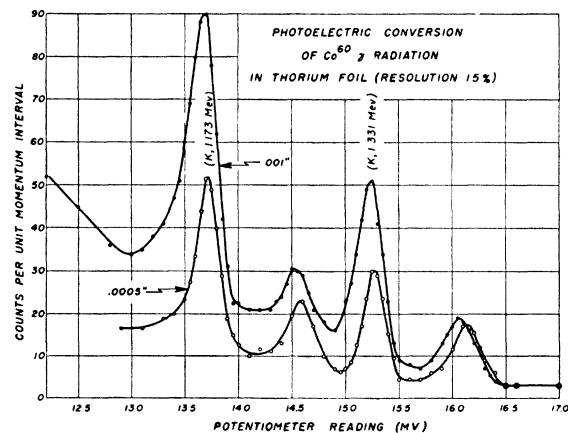
††† Using as a calibration  $B\rho/M.V. = 47.34 \pm 0.3$ .

minations more difficult than the location of the peak. As has already been pointed out, if peak values are to be used, allowance must be made for the converter effects. The corrections to be applied may be roughly estimated from consideration of the effect of folding the window curve into the characteristic primary distribution. For "thin" converters, in which the energy loss is small compared to the resolution width, Jensen, Laslett, and Pratt<sup>16</sup> have pointed out that, if straggling is neglected, this distribution can be approximated by a rectangle of width equal to the average energy loss in the foil, and that the resulting peak shift is one-half this width. The straggling in energy loss due to the relatively infrequent close collisions is, however, an appreciable factor, and will have the effect of spreading the electron distribution on the low energy side. Since the "average" energy loss is heavily weighted by the small fraction of electrons which have lost large amounts of

FIG. 6. 717 kev radiation from  $\text{Be}^9(d,n)\text{B}^{10*}$ , converted in various thorium foils.<sup>16</sup> Jensen, Laslett, and Pratt, Phys. Rev. **75**, 458 (1949).

energy and which thus will have little influence on the peak location, it would seem reasonable that the effective width of the distribution is better measured by the "most probable" energy loss, which gives more equitable weighting to the majority of the electrons. Values of the most probable energy loss in thorium have been calculated for the thicknesses used in these experiments, by R. F. Christy and E. R. Cohen,<sup>17</sup> and the resulting shift limits are shown in Fig. 11 by the three dashed curves extending horizontally to the right; the upward trend at low energies reflects to some extent the influence of scattering in increasing the effective path length. The importance of straggling effects even in the region from 1 to 3 Mev may be judged from the fact that these shift limits are about a factor of two lower than those corresponding to the average energy loss.

For thicker foils, or lower energies the scattering may reach such proportions that many of the photoelectrons produced will become essentially diffused and will either be lost completely or suffer so large energy degradation as to fail to appear in the observed part of the spectrum. The plural scattering and diffusion of electrons has been treated theoretically by Bothe<sup>18</sup> and by Bethe, Rose, and Smith<sup>19</sup> who find that the number of electrons penetrating a given thickness of material drops off very rapidly for thicknesses of the order of the "transport mean free path," which is defined as the distance in which the root mean square scattering angle becomes of the order of  $\pi/4$ . By associating a most probable energy loss with the effective path length for electrons originating at various depths in the converter, one obtains a distribution which decreases monotonically from a maximum at zero energy loss to half intensity at a value corresponding roughly to the most probable energy loss in the transport mean free path. The folding of the window curve into such a spectrum leads to a peak shift approximately equal to the half

FIG. 7. 1.17 and 1.33 Mev gamma-radiation from  $\text{Co}^{60}$ , converted in .0005-inch and .001-inch thorium foils.<sup>17</sup> R. F. Christy and E. R. Cohen (to be published).<sup>18</sup> W. Bothe, Zeits. f. Physik **54**, 161 (1929).<sup>19</sup> Bethe, Rose, and Smith, Proc. Am. Phil. Soc. **78**, 573 (1938).

width at  $1/e$  of the maximum (0.60 times the full width at half maximum) of the window curve. This limit, indicated by the dashed diagonal line of Fig. 11, is quite insensitive to the detailed shape of the primary distribution and should give a fairly reliable upper limit to the shift in the energy range 0.2 to 1.0 Mev for resolution widths less than about 5 percent. This line represents then the limiting case of an infinitely thick converter which together with the "thin" converter limit accounts for the main feature of the curves of Fig. 11. A somewhat more detailed treatment, assuming an exponential distribution cut off sharply at the most probable energy loss, for intermediate converter thicknesses leads to the solid curves of Fig. 11. The coefficient of the exponential was taken as inversely proportional to the energy loss in a transport mean free path, the constant of proportionality having been adjusted to fit the experimentally determined shifts for  $Au^{198}$  and annihilation radiation. The limiting cases of thick and thin converters exhibited in these curves merge reasonably well into the limits indicated by the more general considerations.

The extent to which the above discussed effects are applicable may be seen, at least qualitatively from the distributions of Fig. 5 and Fig. 8. Photoelectrons that are produced at a depth within the converter such that the most probable energy loss suffered in emerging from the foil is less than approximately the resolution of the spectrometer will be the most effective in determining both the location and the intensity of the observed line peak. In the present case this amounts to energy losses

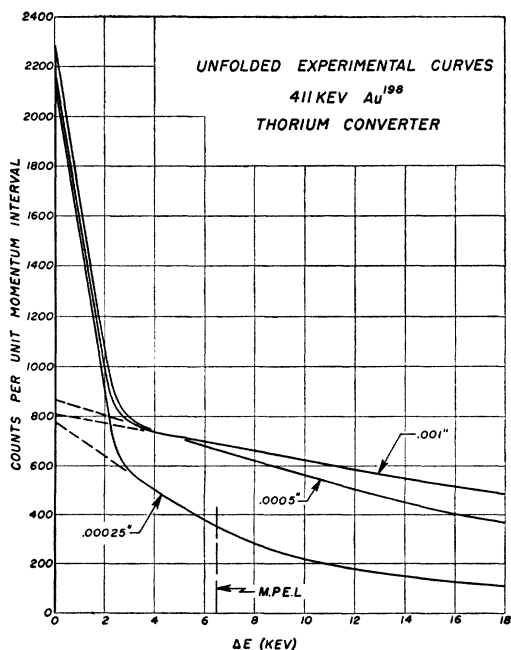


FIG. 8. Inferred "primary" distribution in energy of photoelectrons emerging from thorium converters irradiated by 411 kev  $Au^{198}$  gamma-radiation, as would be observed with infinitely high resolution.

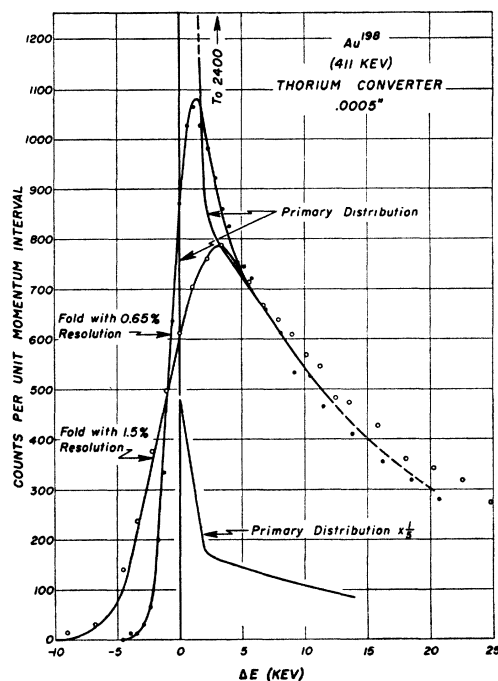


FIG. 9. Inferred primary distribution of photoelectrons produced by 411 kev  $Au^{198}$  radiation in .0005-inch thorium foil. The theoretical "folds" with 1.5 percent and 0.65 percent Gaussian window curves are compared with the observed points.

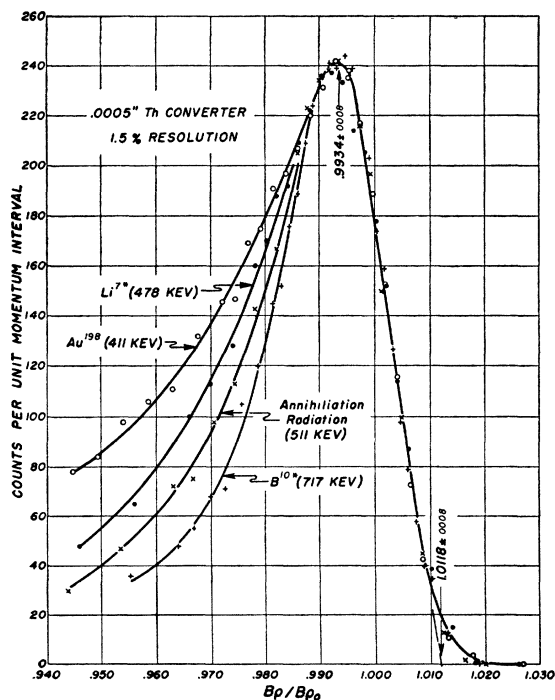


FIG. 10. Observed  $K$  photoelectron distributions for several gamma-rays, converted in .0005 inch thorium. The abscissa  $B_p/B_{p0}=1.000$  corresponds to the true momentum of the photoelectrons, i.e., the expected peak location for an infinitely thin converter.

TABLE IV. Peak determinations, .0005-inch thorium converter.

$\gamma$ -Ray source	Line	M.V.† (current)	$B\rho$ †† (Gauss-cm)	$E_e$ (kev)	$E_e + E_{K,L}$ (kev)	Shift (kev)	$E_\gamma$ (kev)
Au <sup>198</sup> decay	K	43.67	2092.9	298.2	408.0	3.2	411.2
Li <sup>7*</sup>	K	49.50	2372.3	364.8	474.6	(3.8)	478.4 ± .9
Au <sup>198</sup> decay	L	51.38	2462.4	386.9	407.0	4.2	411.2
e <sup>+</sup> annihilation	K	52.24	2503.6	397.1	506.9	3.9	510.8
B <sup>10*</sup>	K	68.77	3295.8	601.4	711.2	(4.9)	716.1 ± 1.3
Co <sup>60</sup> decay (a)	K	103.2 <sub>e</sub> ††	4949	1058. <sub>2</sub>	1168. <sub>0</sub>	(4.2)	1172. <sub>2</sub> ± 2.5
Co <sup>60</sup> decay (b)	K	114.9 <sub>f</sub>	5509	1217. <sub>8</sub>	1327. <sub>6</sub>	(4.0)	1331. <sub>6</sub> ± 2.9

† Corrected for axial component of stray fields.

†† Values reduced to standard shunt reading.

††† Using as a calibration  $B\rho/M.V. = 47.92 \pm .03$ .

less than 8 kev or a depth less than about .0003 inch of thorium. Thus it is observed that the increase of the peak intensity in going from .00025 inch to .0005 inch is comparatively slight although a shift in the location of the peak to a lower energy is apparent. Increasing the foil thickness beyond the "resolution depth" should however materially increase the prominence of the tail just below the peak until a thickness comparable to the transport mean free path is reached. The transport mean free path is estimated to be .0004 inch for this energy. After a thickness of the order of two or three times this value is reached, very few additional electrons are observed even in the tail. The "cut-off" used in the theory is indicated in Fig. 8 for the .00025-inch foil thickness. The absence of any sharp discontinuity in the .00025-inch curve at this energy loss emphasizes the approximate nature of the theory used in obtaining the curves of Fig. 11.

In Table IV are presented the observed peak locations for the various gamma-rays discussed earlier, together with the estimated shift values (in parentheses) taken from Fig. 11. While no great claim to precision can be made in the arguments on which the corrections are based, a comparison with the values of Table III indicates satisfactory agreement between the two sets of determinations. It may be remarked that in the case of the Li<sup>7\*</sup> radiation, the fact that the line is bracketed between two known values makes the determination almost independent of the corrections adduced above. For the Co<sup>60</sup>, a direct extrapolation, ignoring the peak shift would lead to values about 6 kev higher than those quoted in Table IV.

#### DOPPLER SHIFT

In the cases of the Li<sup>7\*</sup> and B<sup>10\*</sup> radiations, an appreciable correction for Doppler effect is involved in the determination of the energy of the excited state because of the center of mass motion. The shift associated with a center of mass velocity along the spectrometer  $v$  is, neglecting effects of order  $v^2/c^2$  and assuming isotropic disintegration,

$$\delta = (v/c)E_\gamma \langle \cos\theta \rangle$$

where  $\langle \cos\theta \rangle$  is the mean cosine of the angle between the

spectrometer axis and the gamma-rays producing photoelectrons in the acceptance cone. An estimate of  $\langle \cos\theta \rangle$  can be made if the scattering of the photoelectrons is neglected and if the angular distribution of the photoelectrons is simply taken to be a delta-function at the angle

$$\omega = \cos^{-1}\beta_e$$

with the direction of the gamma-ray, where  $\beta_e$  is the velocity of the photoelectron in units of the velocity of light. Then for the geometry in question, with  $\theta_0$  the acceptance angle of the spectrometer

$$\langle \cos\theta \rangle = [\cos(\theta_0 + \omega)\cos(\theta_0 - \omega)]^{1/2}$$

Table V gives the calculations leading to the values of  $\delta$ , assuming that the residual nucleus has not been stopped before the emission of the gamma-ray. The scattering experienced by the photoelectrons will in general reduce the Doppler shift, since radiation emitted at large angles to the center of mass motion will contribute appreciably to the spectrum. In an experimental comparison of the gamma-ray from the decay of Be<sup>7</sup> with that accompanying the inelastic scattering of protons by Li<sup>7</sup>, the Doppler shift was found to be 1.6 kev<sup>20</sup> for the same geometrical arrangement used here.

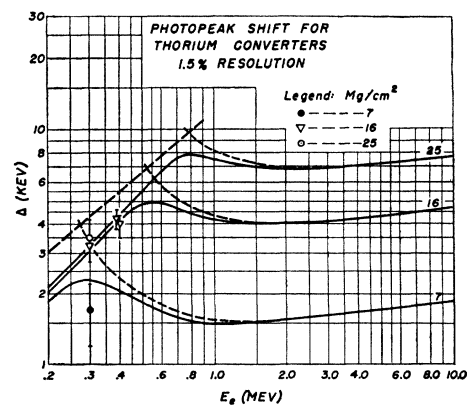


FIG. 11. Peak shift correction for converter thickness as a function of initial photoelectron energy.

<sup>20</sup> Rasmussen, Lauritsen, and Lauritsen, Phys. Rev. 75, 199 (1949).



TABLE V. Doppler shifts.

Reaction	Bombarding voltage (Mev)	$v/c$	$\omega$	$\langle \cos\theta \rangle^\dagger$	$\delta$ (keV)
Li <sup>7</sup> (p p')Li <sup>7*</sup>	1.05	.0059	38.5°	.78	2.2
Be <sup>9</sup> (d n)B <sup>10*</sup>	.96	.0058	27.1°	.86	3.6

†  $\theta_0 = 13^\circ$ .

The calculated shift for B<sup>10\*</sup> has been reduced by the same proportion in the computation of the final values, even though at this higher energy the scattering is certainly less important. Table VI presents the final values, using the means of Tables III and IV, and including the estimated Doppler shifts.

The present value for the excited state of Li<sup>7</sup> is slightly lower than the value  $478.5 \pm 1.5$  keV given by Elliott and Bell<sup>21</sup> for B<sup>10</sup>(n $\alpha$ )Li<sup>7\*</sup> but as the probable errors overlap, the difference is hardly significant. The Co<sup>60</sup> values are about 15 keV higher than those obtained by Jensen, Laslett, and Pratt<sup>16,\*</sup>; the reason for

<sup>21</sup> L. G. Elliott and R. E. Bell, Phys. Rev. **74**, 1869 (1948).

\* Note added in proof: More recent work by the authors, kindly communicated to us by Professor Laslett has led to values which, when adjusted by use of the average energy loss, agree well

TABLE VI. Gamma-ray and excitation energies.

Reaction	$E_\gamma$ (keV)	$\delta$ (keV)	$\Delta E_{\text{level}}$ (keV)
Li <sup>7</sup> (p p')Li <sup>7*</sup>	$478.3 \pm .6$	$1.6 \pm .7$	$476.7 \pm .9$
Be <sup>9</sup> (d n)B <sup>10*</sup>	$716.4 \pm .8$	$2.6 \pm 1.0^\dagger$	$713.8 \pm 1.3$
Co <sup>60</sup> ( $\beta^-$ )Ni <sup>60*</sup> (a)	$1172.4 \pm 1.8$	0	$1172.4 \pm 1.8$
Co <sup>60</sup> ( $\beta^-$ )Ni <sup>60*</sup> (b)	$1330.9 \pm 2.1$	0	$1330.9 \pm 2.1$

† Taken as  $\approx 1.6/2.2 \times 3.6$ .

this discrepancy is not clear. A preliminary crystal spectrometer determination of these lines, kindly communicated to us by Professor DuMond and Dr. Lind is in good agreement with the values quoted here.

It is a pleasure to acknowledge the many helpful suggestions and active assistance of Professor R. F. Christy in connection with this problem. We are also indebted to Professors C. C. Lauritsen and W. A. Fowler for valuable advice and consultations. This work was assisted by the joint program of the ONR and the AEC.

with those cited here. The agreement is less good if the shift is calculated from the most probable energy loss, but is still within the combined probable errors.

## Penetration and Diffusion of X-Rays through Thick Barriers. II. The Asymptotic Behavior when Pair Production Is Important\*

U. FANO

National Bureau of Standards, Washington, D. C.

(Received May 16, 1949)

The methods of a previous paper are modified to cover the high energy x-rays which are strongly absorbed by pair production. The variation of intensity with depth of penetration is then expected to follow a law of the type  $x^{-5/6} \exp(-\mu_m x + bx^3)$ .

THE factors governing the approach to spectral equilibrium in the penetration of hard x-rays have been discussed in a previous paper,<sup>1</sup> which will be referred to as I. It was found that the trend of the total x-ray intensity at great depth of penetration depends essentially upon the progressive formation and decay of those secondary components that are least absorbed.†

The earlier treatment assumed that the primary

\* Work supported by the Applied Mathematics Branch of the ONR.

<sup>1</sup> Bethe, Fano, and Karr, Phys. Rev. **76**, 538 (1949).

† Note added in proof: The results derived in I are closely related to those derived by Wick (Phys. Rev. **75**, 738 (1949)) in his treatment of the analogous neutron problem. Wick also took into account the effect of small angular deflections and his methods are now being applied to the x-ray problem. This effect tends to modify the values of the constants in (13 a and c) without changing the structure of these formulas. Finally, it is understood that some of the results reported in I were also obtained by Greuling (unpublished).

x-rays are less absorbed than any of their secondaries. This obtains in lead only up to energies of about 3 Mev, in lighter elements up to higher energies. At very high energies absorption by pair production becomes increasingly important and secondary scattered x-rays may be more penetrating than the primaries. Under these conditions the softer x-ray components still approach an equilibrium, but this equilibrium state is now controlled by the formation and decay of the hardest secondary components. The energy of these components corresponds to the minimum of the plot of absorption coefficient vs. photon energy,<sup>2</sup> and may be much lower than the energy of the primaries. (The present analysis disregards the bremsstrahlung of the electrons generated by pair production.)

<sup>2</sup> See, e.g., W. Heitler, *Quantum Theory of Radiation* (Oxford University Press, London, 1944), p. 216.